



Photocatalytic water disinfection under solar irradiation by Ag@TiO₂ core-shell structured nanoparticles



S. Sreeja, Vidya Shetty K*

Department of Chemical Engineering, National Institute of Technology Karnataka, Surathkal, Srinivasnagar Post, Mangalore 575025, India

ARTICLE INFO

Article history:

Received 23 January 2017

Accepted 19 July 2017

Available online 17 August 2017

Keywords:

Ag@TiO₂ core shell nanoparticles

Endotoxin

Solar photocatalysis

Water disinfection

ABSTRACT

The Ag core-TiO₂ shell structured (Ag@TiO₂) nanoparticles were found to be efficient in the disinfection of water under solar light irradiation both in free and immobilized form. Complete disinfection of 40 × 10⁸ CFU/mL *Escherichia coli* cells was achieved in 15 min by solar photocatalysis with 0.4 g/L Ag@TiO₂ catalyst loading. Ag@TiO₂ nanoparticles were found to be superior to TiO₂ nanoparticles in solar disinfection. Photocatalysis rate was found to increase with increase in catalyst loading and with decrease in cell concentration. Ag@TiO₂ nanoparticles showed their efficacy in the degradation of endotoxin, a harmful disinfection byproduct. Kinetics of solar disinfection with Ag@TiO₂ nanoparticles followed Chick's law. The kinetics of endotoxin degradation followed zero order kinetics at high concentrations of endotoxin. However at lower concentrations, rate followed a nth order model with n = 6.99. A lower rate of photocatalytic disinfection with Ag@TiO₂ nanoparticles immobilized on cellulose acetate as compared to that in their free form was observed, owing to diffusional and light penetration limitations. The re-growth of cells after photocatalytic disinfection was below the detectable limits, thus proving the potential of the process to produce safe drinking water. Ag@TiO₂ nanoparticles can find potential application in solar water disinfection and the process which harnesses the solar energy may prove to be energy efficient and economical, thus can be easily adopted for large scale applications and portable drinking water treatment units for domestic applications.

© 2017 Elsevier Ltd. All rights reserved.

1. Introduction

Water is the most imperative resource needed for life sustainability. Availability of safe and good quality drinking water is a basic need and is scarce, in most of the developing and under developed countries (WHO, 2014). Traditional methods of water purification include processes such as sedimentation, boiling, filtration, chlorination, ozonation and others. However, usage of such methods involves high operating costs and the formation of harmful disinfection byproducts (Qilin et al., 2008; Richardson et al., 2007). To circumvent these problems the use of advanced oxidation process came into existence. Matsunaga et al. (1985) proposed TiO₂ as a photocatalytic disinfectant to inactivate *Lactobacillus acidophilus*, *Saccharomyces cerevisiae*, and *Escherichia coli*. Lanoa et al. (2010, 2012) have also shown bacterial inactivation by photocatalysis using TiO₂. However, TiO₂ is active under shorter wavelength radiation owing to its high band gap energy of 3.2 eV (Gamage, 2014), and the ability of TiO₂ to effectively use natural sunlight is limited. Higher rate of electron-hole recombination with TiO₂

(Choi et al., 1994) is also disadvantageous in terms of lower rate of photocatalysis. Recombination of electrons and holes reduces the probability of formation of active radicals which bring about photocatalysis (Sclafani and Herrmann, 1996)

Solar energy is a highly economical and easily available form of energy known to mankind. The oldest method of water purification using sunlight dates back to 2000 BCE. Nonetheless, it is only in more recent times that water purification by sunlight has been systematically evaluated. Acra et al. (1980) at the American University in Beirut projected the practical application of sunlight for the disinfection of drinking water and described the process as solar disinfection or SODIS. Solar water disinfection is widely used. However the disadvantage of this process includes factors such as turbidity of water, seasonal variations, longer inactivation time and bacterial regrowth (Ibáñez et al., 2015; Sciacca et al., 2011; Gelover et al., 2006; Meierhofer and Wegelin, 2002). Optimum growth temperature of the microorganisms can have an antagonistic effect on solar disinfection and slow down the process (Vivar et al., 2017). To improve the efficacy of the process, TiO₂ coated surfaces were used, where photocatalysis serves as a purification process thereby making it useful for drinking purposes (Meierhofer and Wegelin, 2002). However the ability of TiO₂ to

* Corresponding author.

E-mail addresses: vidyaks68@yahoo.com, vidyaks95@nitk.ac.in (V. Shetty K).

effectively use natural sunlight is limited due to its high band gap energy of 3.2 eV (400 nm) (Gamage, 2014). The inability of TiO₂ in its application under solar light can be overcome by the use of composite structures with TiO₂ (Markad et al., 2017), metal doping, or core shell structures of metal and TiO₂ (Kedziora et al., 2012; Li and Li, 2001; Liga et al., 2011; Mai et al., 2010; Pratap Reddy et al., 2007; Sumana et al., 2013). One such engineered approach was done by Khanna and Shetty (2013, 2014, 2015) using Ag metal core and TiO₂ as the shell wherein the band gap energy was lowered (Khanna, 2014). The synthesis of Ag@TiO₂ nanoparticles for effective utilisation of UV light and sunlight was done by Khanna and Shetty (2013, 2014, 2015) for degradation of dyes, and these nanostructures have been reported to be effective in phenol degradation under UV and solar light (Shet and Shetty, 2015; 2016), water disinfection under UV light (Sreeja and Shetty, 2016). The present study reports the solar light mediated water disinfection using Ag@TiO₂ nanoparticles. Nanoparticles with silver core and TiO₂ shell can offer advantages as photocatalysts due to distinctive properties such as electron charge transfer and surface plasmon resonance (Hirakawa and Kamat, 2005) thereby promoting effective separation of photogenerated electron – hole pair which may lead to enrichment of photocatalytic efficiency of Ag@TiO₂ nanoparticles.

The mechanism underlying the photocatalytic disinfection process mainly involves the formation of reactive oxygen species which attack the bacterial cell wall causing lipid peroxidation thereby leading to cell damage and cell death (Maness et al., 1999). The disinfection byproduct, endotoxin is harmful as it shows multiple injurious biological activities (Miyamoto et al., 2009). This paper reports the application of Ag@TiO₂ nanoparticles as photocatalysts for the inactivation of *E. coli* under solar light irradiation and the comparison of photocatalytic efficacy with that of TiO₂ nanoparticles. The effects of catalyst loading, initial cell concentration and sunlight intensity were studied and the kinetics of disinfection and endotoxin degradation are reported.

2. Materials and methods

2.1. Microorganism used as a model pathogen

Esterichia coli (NCIM No. 2350; ATCC No. 8134) was used as a model pathogen and was procured from NCIM (National Collection of Industrial Micro Organisms), Pune, India.

2.2. Preparation of Ag@TiO₂ nanoparticles

Ag@TiO₂ nanoparticles were synthesised using one pot synthesis method of hydrolysis of Titanium-(triethanolaminato) isopropoxide (Sigma-Aldrich, Bangalore, India) in 2-propanol (Merck (India) Ltd, Mumbai, India) and the reduction of silver ions from aqueous AgNO₃ (Merck (India) Ltd, Mumbai, India) using dimethyl formamide (Merck (India) Ltd, Mumbai, India) with molar ratio of Ag to Ti in the synthesis mixture as 1:1.7 and with calcination temperature of 450 °C, following the methodology adopted by Khanna and Shetty (2013).

2.3. Immobilisation of nanoparticles using cellulose acetate

Ag@TiO₂ nanoparticles were immobilised in cellulose acetate film using the methodology reported by Wu et al. (2005) with further modifications (Sreeja and Shetty, 2016; Shet and Shetty, 2016). 1.2 g of cellulose acetate and 10 mL of acetone were mixed well and 0.04 g of the catalyst was added followed by mixing. The thick paste thus formed was cast on a glass petri dish, allowed for

evaporation of acetone and further dried for 15 min in oven. The film was further cut into flakes of 1 cm × 1 cm and used for photocatalytic experiments with immobilized nanoparticles.

2.4. Preparation of *E. coli* cell culture

E. coli cells were grown in 100mL nutrient broth (HiMedia, Mumbai, India) at 37 °C and 150 rpm in a rotary incubator shaker for 12 h. Microbial culture in stationary phase having viable cell count of nearly 10⁸ CFU/mL was centrifuged at 10,000 rpm for 5 min and the pellet was washed with sterilized water. The process of Centrifugation and washing was repeated to remove the nutrient traces on the cell pellet. The cell pellet was re-suspended in 100 mL sterilized water and the cell culture with the required cell count was prepared by suitable dilutions for disinfection studies (Sreeja and Shetty, 2016).

2.5. Photocatalytic disinfection studies

100 mL of *E. coli* culture containing the known cell count as required for the experiment was taken in a 250 mL conical flask and required amount of catalyst was added. This reaction mixture was kept under continuous stirring conditions using a magnetic stirrer. The reactor set-up was placed in open terrace. Experiments were conducted in the month of March and April 2015 in the town of Surathkal, Mangalore, India and the average visible light intensity was measured by LUX meter (KM-LUX-100 K). The initial pH of the reaction mixture was 7 ± 0.5. The conical flask was placed inside a glass beaker with the moist sterilized cotton at the bottom portion, in the space between the beaker and conical flask, such that the temperature of the reaction mixture was maintained at 30.5 ± 1.5 °C throughout the period of the experimental duration. 1mL of sample was collected from the reactor after desired time intervals, suitably diluted for the estimation of viable cell count. The disinfection experiments were also performed with the nanoparticles under dark conditions (in the absence of solar irradiation); in the absence of nanoparticles under solar irradiation and in the absence of nanoparticles under dark conditions. All the experiments were carried out in triplicates, and mean values were used for analysis, at each interval of time.

2.6. Estimation of viable cell count

20 µL of the suitably diluted samples from disinfection experiments were plated on nutrient agar plates in duplicates and incubated at 37 °C overnight. The colonies were then counted and the viable cell concentration was determined in CFU/mL (Sreeja and Shetty, 2016). The percentage disinfection was calculated by finding the difference in initial cell concentration and the cell concentration at any time as a percentage of initial cell concentration (Sreeja and Shetty, 2016)

2.7. Determination of endotoxin concentration

10 µL of samples collected from the reactor during photocatalytic disinfection experiments were refrigerated overnight at –20 °C to stop any bacterial activity. The samples were suitably diluted and the concentration of endotoxin was measured (Sreeja and Shetty, 2016) by Limulus ameocyte lysate (LAL) assay (Tanaka et al., 1992) using Pierce LAL Chromogenic Endotoxin Quantitation Kit (Thermo-Scientific) by comparing with standard endotoxin solution (*E. coli* 011:B4).

3. Results and discussion

3.1. Solar photocatalytic disinfection of water by Ag@TiO₂ nanoparticles

To validate the photocatalytic activity of Ag@TiO₂ under solar light in terms of photocatalytic disinfection of water, the photodegradation of *E. coli* was studied for the following cases (i) in the presence of light and catalyst to test for photocatalysis. (ii) in the presence of light and absence of catalyst to test for possible photolysis by solar light (uncatalyzed) (iii) in the presence of catalyst and absence of light to test for possible bactericidal activity of the nanoparticles and (iv) in the absence of both catalyst and light to test for possible bacterial death. The batch experiments for disinfection were conducted using bacterial suspensions having an initial viable cell concentration of 40×10^8 CFU/mL. The experiments were conducted under solar irradiation of average light intensity of 970×10^2 lux throughout the period of experimentation. The experiments were carried out from 10.30 AM to 12.30 PM (Indian Standard Time) in the month of March 2015. Fig. 1 presents the time course variation of percentage disinfection for all the four cases.

As observed in Fig. 1, complete disinfection of *E. coli* infected water had occurred within 40 min owing to the photocatalytic activity of Ag@TiO₂ nanoparticles. It can be observed from Fig. 1 that in the absence of catalyst and presence of light, 78% disinfection has been achieved at the end of 120 min. Only 30% disinfection occurred in 40 min in the absence of the catalyst. This can be attributed to disinfection by photolysis with UV rays from solar light causing the bacterial cell lysis (Wegelin et al., 1994). The rate of disinfection with solar light has been enhanced by the presence of catalyst, as compared to that in the absence of the catalyst. This faster rate is due to the rapid release of OH[•] during photocatalysis which weakens the self defense mechanism of the bacteria thereby leading to loss of cell respiration and death (Maness et al., 1999). It clearly shows that the photolytic disinfection reaction is effectively catalyzed by Ag@TiO₂ nanoparticles, thus proving their photocatalytic efficacy for water disinfection. In the presence of nanoparticles and absence of solar irradiation, 67% disinfection is seen in 120 min of irradiation and only around 25% has occurred in 40 min, which can be due phagocytosis by nanoparticles (Huang et al., 2000) and also due to the antimicrobial activity of Ag and TiO₂ nanoparticles thereby leading to disintegration of the cell membrane (Guzmán et al., 2009; Piskin et al., 2013). In the con-

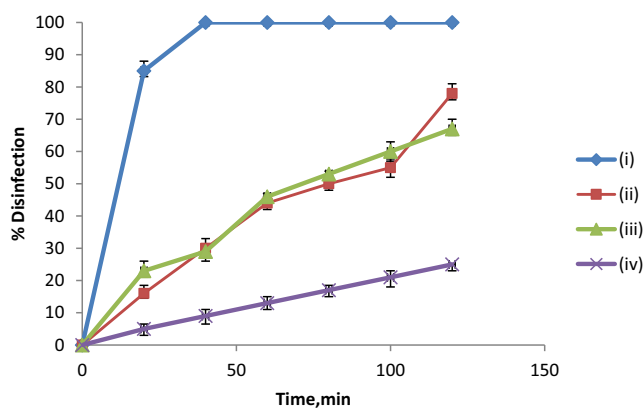


Fig. 1. Disinfection studies (i) in the presence of light and catalyst (catalyst loading = 0.3 g/L), (ii) in the presence of light and absence of catalyst, (iii) in the presence of catalyst (catalyst loading = 0.3 g/L) and absence of light, and (iv) in the absence of catalyst and light. Average initial viable cell concentration = 40×10^8 CFU/mL.

trol/dark experiment i.e. the absence of both light and Ag@TiO₂, a mere 25% disinfection was seen after 120 min of irradiation, which could possibly be because of the absence of nutrient source for survival. On comparison from Fig. 1, it can be concluded that the disinfection is occurring mainly due to photocatalytic effect which is caused by the Ag@TiO₂ nanoparticles and thus proving Ag@TiO₂ nanoparticles to be efficient photocatalysts for water disinfection under solar light.

3.2. Effect of initial cell concentration

Inactivation of a bacterial population is considered to be a function of viable cells remaining in the system (Pham et al., 1997). Increased cell concentration may also increase the turbidity of the solution which is known to influence the photocatalytic efficiency of the process (Meierhofer and Wegelin, 2002). The efficacy of the catalyst for effective inactivation of *E. coli* was studied by varying the initial cell concentration from 10^4 to 10^8 CFU/mL in the reaction mixture and keeping the catalyst loading constant at 0.1 g/L. The experiments were conducted for 35 min of irradiation with the average solar light of intensity 1040×10^2 lux and the temperature was maintained at 30.5 ± 1.5 °C throughout the period of experimentation. The experiments were conducted between 12.00 Noon and 12.35 PM (IST) in the month of March 2015. Fig. 2 presents the variation of percentage disinfection with time during photocatalysis at various initial cell concentrations. These experiments were conducted with a lower catalyst loading of 0.1 g/L, as when higher catalyst loadings were used with cell concentrations of $<10^8$ CFU/mL, the photocatalysis occurred at a very fast rate making it difficult in analysis.

Fig. 2 shows the effect of initial cell concentration on the photocatalytic activity of Ag@TiO₂ for water disinfection. Highest cell concentration used was around 40×10^8 CFU/mL wherein only 80% disinfection was achieved at the end of 35 min and an increased exposure time of 60 min resulted in complete inactivation (data not shown). However with decreased initial bacterial concentrations, the disinfection rate increased and 100% disinfection was achieved within 35 min for bacterial loading of 10^7 – 10^4 CFU/mL. The hindered photocatalytic activity at higher concentrations can be accounted for the insufficient production of ROS in the short time interval needed for disinfection of such a large number of cells, owing to fixed number of active sites provided by the catalyst. Higher cell concentrations lead to the turbidity in the reactor content, which may act as a barrier for light penetration thereby diminishing the light exposure to the nanoparticles leading to its reduced photocatalytic activity. Inactivation time of as low as 10 min was sufficient to disinfect water

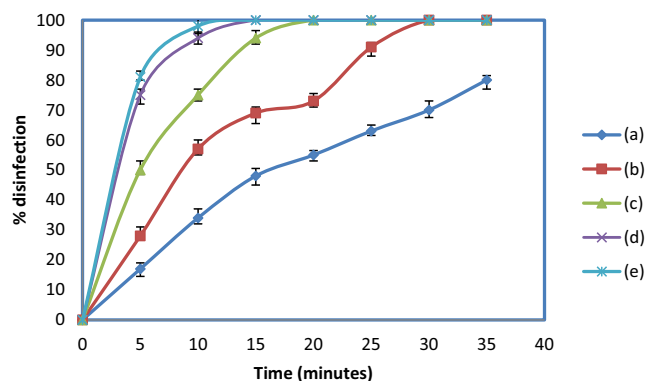


Fig. 2. Effect of initial cell concentration on the percentage disinfection of *E. coli*. Catalyst loading = 0.1 g/L, initial cell concentrations used are (a) 10^8 CFU/mL, (b) 10^7 CFU/mL, (c) 10^6 CFU/mL, and (d) 10^5 CFU/mL (e) 10^4 CFU/mL.

with 10^4 CFU/mL cell concentrations. This result is in agreement with results obtained by Bekbölet (1997) and Sunada et al. (2003) wherein disinfection rate was reported to be increased with decreased cell concentration which can be associated with lower turbidity and sufficient generation of ROS thereby providing effective disinfection and higher photocatalytic activity. Prolonged exposure times may be recommended when the bacterial population density is larger to achieve effective disinfection with lower catalyst loading.

3.3. Kinetics for disinfection

Evaluation of kinetics of disinfection facilitates the assessment of disinfection performance and the design of contactors for microbial disinfection (Gyiirek and Finch, 1998). The kinetics of the complex disinfection mechanism is often represented by the classical Chick's model which is widely used to evaluate the kinetics (Chick, 1908). Chick's law (Eq. (1)) assumes that the rate is first order with respect to cell concentration (Gyiirek and Finch, 1998).

$$\frac{dN}{dt} = -kN \quad (1)$$

where N is the cell concentration in CFU/mL, t is the time of disinfection and k is the rate constant

Further the general expression for this model is given by Eq. (2)

$$\ln \frac{N}{N_0} = -k * t \quad (2)$$

In the present work, the applicability of the Chick's model has been assessed for the evaluation of the kinetics for photocatalytic disinfection. The cell-concentration-time data obtained during photocatalysis by batch experiments conducted with $40 * 10^8$ CFU/mL initial cell concentration and Ag@TiO₂ catalyst loadings of 0.1 g/L was used to test the validity of the kinetic model.

The plot of log survival ratio v/s time shown in Fig. 3 gives a linear fit with the goodness of fit being indicated by the R^2 value of 0.9886 which is closer to 1 as shown in Fig. 3. The good fit of the model validates the hypothesis and theories as stated in the Chick's model. The pseudo first order rate constant was obtained from the slopes of the line and was found to be 0.0426 min^{-1} for catalyst loading of 0.1 g/L and average light intensity of $1040 * 10^2$ lux.

3.4. Effect of catalyst loading

The photocatalytic degradation efficiency depends on the concentration of both the target compound and the catalyst concentra-

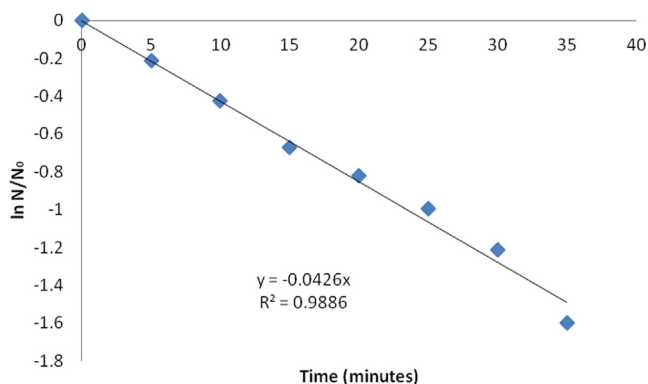


Fig. 3. Chick Watson model fit for the photocatalytic disinfection with 0.1 g/L of Ag@TiO₂ catalyst loading.

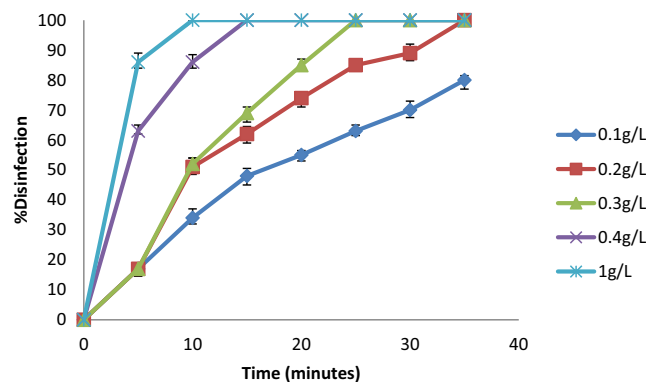


Fig. 4. Effect of catalyst loading on the percentage disinfection. Average light intensity = $998 * 10^2$ lux.

(Habibi et al., et al., 2005). It also aids in the economics of the process and effective use of reactor space (Ibhadon and Fitzpatrick, 2013). The experiments on the effect of catalyst loading were performed with an average initial viable cell concentration of $40 * 10^8$ CFU/mL, initial pH of 7 ± 0.5 and with the catalyst loading of 0.1–1 g/L in the month of March between 12.00 PM and 12.35 PM (IST). These experiments were conducted for 35 min with irradiation using solar light of average intensity $998 * 10^2$ lux and the temperature was maintained at 30.5 ± 1.5 °C throughout the period of experimentation. Fig. 4 presents the variation of percentage disinfection with time during photocatalysis with initial cell concentration of 10^8 CFU/mL and varying catalyst loading.

As presented in Fig. 4, maximum photocatalytic activity could be achieved when 1 g/L of Ag@TiO₂ was used wherein 100% disinfection was observed at the end of 10 min. However with decreased catalyst loading a decrease in the disinfection rate was seen. With a low catalyst loading of 0.1 g/L, 80% disinfection occurred at the end of 35 min. However with prolonged exposure time of 60 min, 100% disinfection was achieved (data not shown). In case of 0.2 g/L, 0.3 g/L and 0.4 g/L Ag@TiO₂ loading, 100% disinfection was observed at the end of 35, 25 and 15 min respectively indicating a delay of 10 min in the disinfection rate for a drop of 0.1 g/L catalyst loading. However, an increase in catalyst loading from 0.4 g/l to 1 g/L, decreased the time for complete disinfection only by 5 min, thus catalyst loading of 0.4 g/L has been found to be favorable for the disinfection of water with cell concentration of 10^8 CFU/mL.

These results also show that, there is no proportional correlation between the time for achievement of complete disinfection and the catalyst loading. This may be owing to the two opposing phenomena of increase in surface active sites and hindrance to light penetration effect occurring with increase in catalyst loading. The former tends to increase the rate and later tends to decrease it, and the net effect governs the overall rate. Rincón and Pulgarin (2006) has reported a 100% disinfection using TiO₂ and solar light illuminated systems at the end of 40 min using a catalyst loading of 0.5 g/L and Paleologou et al. (2007) has reported that above 1 g/L catalyst loading, *E. coli* inactivation reached a saturation level which is accounted for weak light penetration into the solution at these high catalyst loadings. Such an effect was not observed in the present study, perhaps due to the fact that relatively low catalyst loadings were used. However, at higher increase in catalyst loading resulted in smaller increase in the rate, showing that the effect of light penetration effect is becoming dominant. Nevertheless, in the present study even at low catalysts loading, *E. coli* photocatalytic inactivation was significantly high with Ag@TiO₂ nanoparticles.

3.5. Comparison of TiO₂ and Ag@TiO₂ photocatalysts

Semiconductors are the most widely used photocatalysts and TiO₂ is a widely used photocatalyst (Gupta and Tripathi, 2011). TiO₂ nanoparticles are generally used as a common reference for photocatalytic activity. Thus the photocatalytic activity of Ag@TiO₂ was compared with that of commercial TiO₂ (Degussa P25) nanoparticles for water disinfection in the present study. The experiments were conducted using 1 g/L catalyst loading, initial cell concentration of 10⁸ CFU/mL and an initial pH of 7 ± 0.5. Fig. 5 presents the comparison of time course variation of percentage disinfection with Ag@TiO₂ and TiO₂ photocatalysts.

As observed in Fig. 5, Ag@TiO₂ is more efficient than TiO₂. Ag@TiO₂ caused 100% disinfection at the end of 10 min while TiO₂ took 35 min for complete disinfection under solar light with the catalyst loading of 1 g/L. This pronounced disinfection efficacy of Ag@TiO₂ can be accounted for the rapid release of hydroxyl radicals in the initial phase by photocatalytic action which acts on cell membrane leading to loss of cell integrity in the preliminary stages of disinfection. This activity of Ag@TiO₂ is due to its low band gap energy (Khanna, 2014) as compared to that for TiO₂ which increases the e⁻-h⁺ charge separation (Khanna and Shetty, 2014; Tunc et al., 2010) and implying that Ag@TiO₂ results in delayed recombination rate (Hirakawa and Kamat, 2004), thereby increasing the rate of photocatalytic disinfection. Ag@TiO₂ has been reported to have a lower band gap energy (Khanna, 2014) as compared to the band gap energy of TiO₂ nanoparticles. Khanna and Shetty (2014) have shown that Ag@TiO₂ nanoparticles can absorb light both in the UV and visible light wavelength range and the maximum absorption under solar light was reported to occur at a wavelength of 509 nm. The results thereby obtained are in concordance with that reported by Khanna (2014) for photocatalysis of Reactive blue-220 dye under UV light irradiation as well as in solar light irradiation (Khanna and Shetty, 2014). These results illustrate the enhanced photocatalytic activity of Ag@TiO₂ as compared to TiO₂ under solar light irradiation. The Ag@TiO₂ nanoparticles synthesized in the current study contained a Ag core and TiO₂ shell with the average size of 37 nm. The Transmission electron microscopic (TEM) image of the particles along with the Energy Dispersive Spectra of Ag@TiO₂ have been reported by Sreeja and Shetty (2016). The present study reveals that the core shell structure imparts good photocatalytic activity in terms of microbial disinfection of water under solar light.

3.6. Endotoxin degradation

Endotoxin is a lipopolysaccharide complex which is an active component of the bacterial cell wall and are covalently linked.

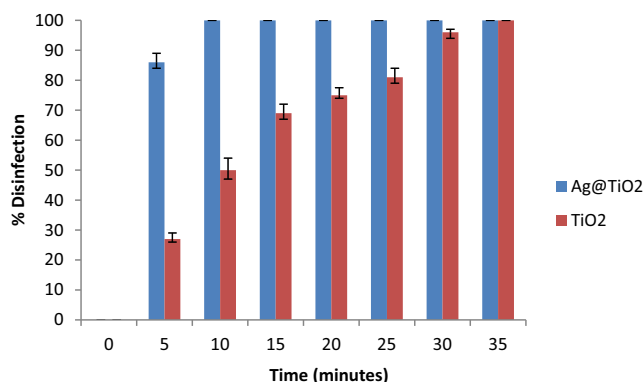


Fig. 5. Comparison of Ag@TiO₂ and TiO₂ photocatalysts; Average light intensity 1110 × 10² lux.

The lipid component causes toxic effects while the polysaccharide unit results in immunogenic responses (Rosenstreich et al., 1973) in humans at very low concentrations (Galanos et al., 1984). The mechanism of disinfection studied previously suggests that this lipid component of the gram negative bacteria undergoes oxidation resulting in the disinfection process (Sunada et al., 1998) thereby releasing the endotoxin into the treated water. As the endotoxin levels in drinking water may lead to certain health effects, the possibility of endotoxin degradation by solar photocatalysis was tested. Experiments were performed with an average initial viable cell concentration of 40 × 10⁸ CFU/mL and with the catalyst loading of 1 g/L. The experiment was conducted for 120 min with irradiation using solar light of average intensity 970 × 10² lux and the temperature was maintained at 30.5 ± 1.5 °C throughout the period of experimentation. The samples were refrigerated at -20 °C to stop any bacterial activity and suitably diluted before use. The samples were analyzed for endotoxin concentration using the LAL assay kit as described in Section 2.7.

From Fig. 6 it is seen that endotoxin levels have reduced from 0.44 EU/mL to 0.121 EU/mL which shows that Ag@TiO₂ nanoparticles can effectively degrade the endotoxins. Around 72% degradation of endotoxin occurred in 120 min. Prolonged exposure to photocatalytic treatment may further reduce the endotoxin levels below the harmful limit. The rates of endotoxin degradation by photocatalysis as a function of endotoxin concentrations were determined by drawing the tangents at various points on the endotoxin concentration vs. time plot and then calculating the slopes of these tangents. The slopes of the tangents yield the rates at particular concentration. The plot of rate vs. concentration is presented in Fig. 7.

From the plot of rate vs concentration of endotoxin shown in Fig. 7, it can be seen that the dependency of rate on concentration falls into two regions. The rate remains constant at high concentrations of endotoxin, showing that the rate is independent of concentration at concentrations at and above 0.25 EU/mL. However in the region below this concentration level, the rate was found to increase with the increase in concentration. This may be attributed to higher number of collisions and the higher fraction of effective collisions of endotoxin molecules on the catalyst surface occurring at higher concentration of endotoxin.

To determine the kinetics of endotoxin degradation in this region, a nth order kinetics shown in Eq. (2) was tested. A plot of ln r vs. ln C was plotted as shown in Fig. 8.

From Fig. 8 it is seen that the plot is linear indicating the validity of nth order model representing the kinetics, wherein k is the rate constant having a value 778.75 (EU/L)^{-5.99}.min⁻¹ and n has a value of 6.99. This implies that the rate of endotoxin degradation follows

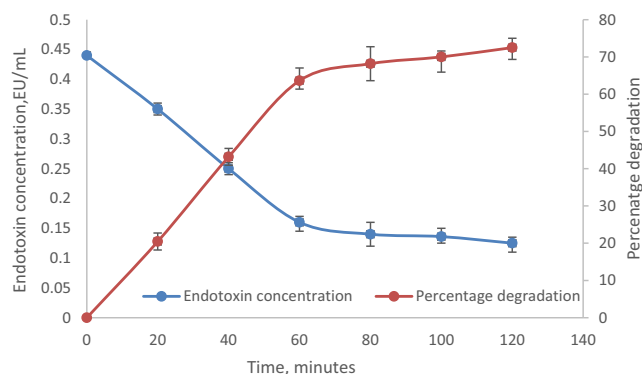


Fig. 6. Photocatalytic degradation of endotoxin using Ag@TiO₂ nanoparticles. Average intensity of solar light 970 × 10² lux.

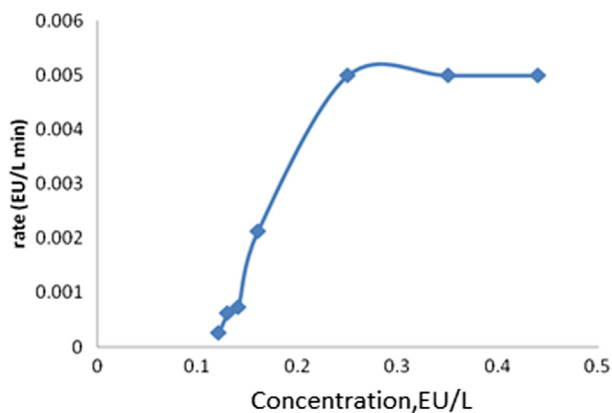


Fig. 7. Kinetic studies for endotoxin degradation using Ag@TiO₂ nanoparticles.

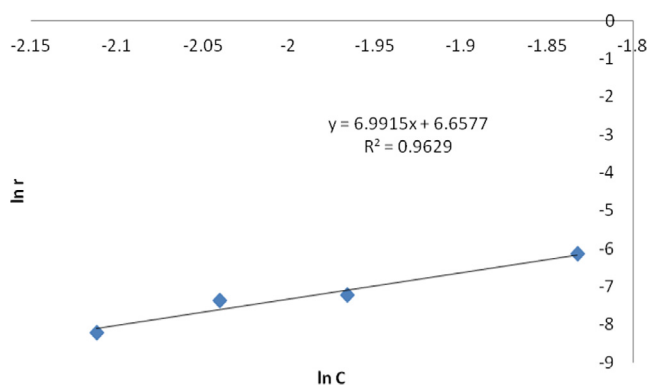


Fig. 8. Fit for kinetics of endotoxin degradation using Ag@TiO₂ nanoparticles at low concentration.

a zero order kinetics at high concentrations of endotoxin, but at lower concentrations rate follows a nth order model of positive order.

3.7. Effect of light intensity

The amount of light that earth receives is dependent on the time of the year and the day. Rincón and Pulgarin (2006) stated that the flow and number of photons generated is directly proportional to the light intensity thereby increasing the bacterial disinfection rate. Light intensity is one of the rate controlling parameters in photocatalysis (Borges et al., 2016). Cho et al. (2004) reported an increase in disinfection rate with an increase in light intensity. Thus, the effect of light intensity on photocatalytic disinfection by Ag@TiO₂ nanoparticles was studied. This was done by exposing the reaction mixture to photocatalytic disinfection at various times of the day in the month of April 2015. The experiments were performed with an average initial viable cell concentration of 40×10^8 CFU /mL, initial pH of 7 ± 0.5 and with the catalyst loading of 0.4 g/L. The experiment was conducted for 35 min of irradiation with solar light at different times of the day and the temperature was maintained at 30.5 ± 1.5 °C throughout the period of experimentation. Fig. 9 presents the variation of percentage disinfection with time during photocatalysis.

From Fig. 9, it can be observed that, disinfection rate is nearly the same during all times of the day. During the morning from 9.30 to 10.05AM and in the evening, 100% disinfection is seen at the end of 20 min, while the complete disinfection occurred within 15 min during mid-day. During mid-day from 1.30 to 2.05 PM, highest efficiency of catalyst was observed. The intensity of light

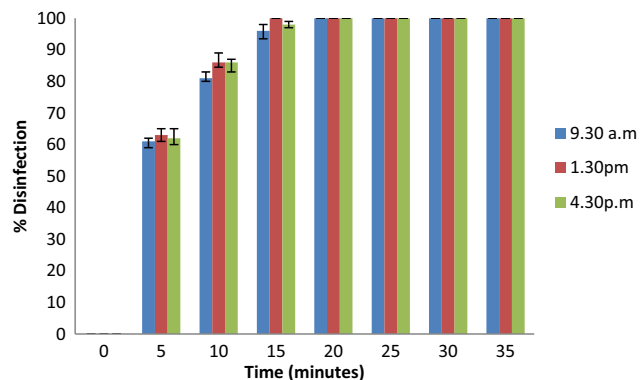


Fig. 9. Effect of light intensity on photocatalytic disinfection at different times of the day (time indicating the start of the experiment) (i) 9.30 a.m, light intensity = 950×10^2 lux, (ii) 1.30 p.m, light intensity = 1110×10^2 lux, and (iii) 4.30p.m, light intensity = 970×10^2 lux.

is the maximum during the mid-day, thus increasing the rate of photocatalysis yielding complete disinfection with less time. Hence it can be concluded that maximum catalyst efficiency was seen during mid-day when sunlight intensity is the highest. However, the dependency of photocatalytic disinfection rate on solar light intensity seems to be marginal, owing to marginal variation in intensities throughout the day in the summer in tropical countries.

3.8. Bacterial recovery test

When growth conditions become favorable, bacteria can re-grow to a viable state even after disinfection and cause disease (Dunlop et al., 2002). Thus it becomes essential to check the survivability of the bacteria post disinfection cycle. In photocatalysis experiment using 0.4 g/L of free catalyst and an initial bacterial concentration of 40×10 CFU/mL, after 100% disinfection was reached, the liquid samples from the reactor at the end of 60 min were cultured for 8, 16, 24,32 and 48 h. The number of viable cells found was below the detectable limits and hence it can be concluded that complete disintegration of *E. coli* had occurred by solar photocatalysis making the treated water safe for use.

3.9. Solar photocatalysis by immobilized Ag@TiO2 nanoparticles

To avoid the challenges in the separation and recovery of nanoparticles post photocatalysis, nanoparticles in immobilized form may prove beneficial. Photocatalysis can be carried out by immobilising nanoparticles on various matrices (Gumy et al., 2006). In the present study the Ag@TiO₂ nanoparticles are immobilized on to a transparent cellulose acetate film. Experiments were performed with an average initial viable cell concentration of 40×10^8 CFU /mL, initial pH of 7 ± 0.5 and with the catalyst loading of 0.4 g/L. Cellulose acetate (CA) flakes prepared with 1.2 g of cellulose acetate containing 0.04 g of Ag@TiO₂ catalyst were used for the batch experiment on photocatalysis with 100 mL reaction media such that the catalyst loading was 0.4 g/L. The experiments were conducted with the immobilized catalyst and bare cellulose acetate flakes for 35 min with irradiation under solar light of average intensity 980×10^2 lux and the temperature was maintained at 30.5 ± 1.5 °C throughout the period of experimentation. Fig. 10 presents the variations of percentage disinfection with time during disinfection with free catalyst, immobilized catalyst and in the absence of catalyst with bare CA flakes.

From Fig. 10, it can be seen that 29% disinfection occurred over a period of 35 min with bare cellulose acetate film flakes, which may

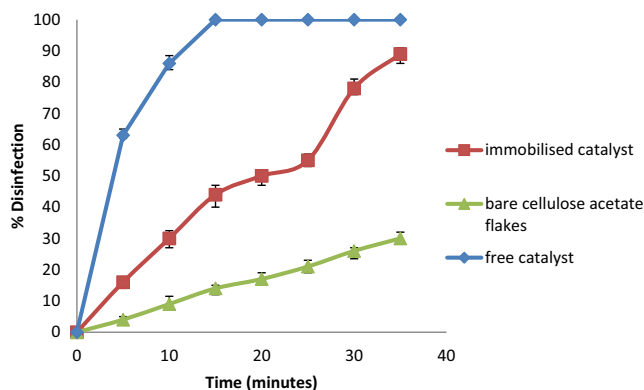


Fig. 10. Effect of immobilization of Ag@TiO₂ nanoparticles on disinfection under solar light for free catalyst, immobilized catalyst and with bare CA flakes. Initial cell concentration = 40×10^8 CFU /mL, catalyst loading = 0.4 g/L.

be attributed to the death of microbes due to lack of availability of nutrient source and due to photolysis in the presence of solar light. In comparison with the result shown in Fig. 1, in the presence of light source without the catalyst and the values obtained for percentage disinfection using bare cellulose acetate, it can be inferred that in the presence of cellulose acetate marginal increase in photocatalytic disinfection was observed. This may be attributed to attachment of a few bacteria on to the film surface and bactericidal activity of Cellulose acetate itself. From Fig. 10, it is observed that photocatalytic disinfection is faster in case of free nanoparticles. However 90% disinfection is seen while using immobilized nanoparticles at the end of 35 min which confirms the photocatalytic activity of immobilized Ag@TiO₂ nanoparticles. The reduced degradation efficiency with immobilized catalysts can be attributed to lack of light penetration to the nanoparticles as they are entrapped in the film, thereby reducing the net photoexcitation capacity of all the nanoparticles present. This reduced photocatalytic activity may also be due to the diffusional mass transfer limitations for the transfer of ROS generated on the surface of the nanoparticles to the bulk solution, to be available for disinfection. Diffusional limitations to oxygen transfer to the surface of nanoparticles may also exist. Regardless of this reduced efficiency of immobilized nanoparticles, it is preferred due to ease of recovery and reduced risk of toxicity of treated water. The drawback in terms of reduced rate of photocatalysis can be however circumvented using higher catalyst loadings.

4. Conclusion

The efficacy of Ag@TiO₂ nanoparticles in the disinfection of water under solar light irradiation was investigated. Ag@TiO₂ nanoparticles were found to be effective photocatalysts for disinfection of water contaminated with *E. coli* under solar light irradiation. Complete disinfection of 40×10^8 CFU/mL was achieved in 15 min for solar photocatalysis with 0.4 g/L catalyst loading. Ag@TiO₂ nanoparticles were found to be superior to TiO₂ nanoparticles in disinfection of water by photocatalysis. Photocatalysis rate was found to increase with increase in catalyst loading. With increase in cell concentration, the photocatalytic activity of Ag@TiO₂ decreased and a change in light intensity was found to have marginal effects in case of solar photocatalysis. Kinetics of solar disinfection with Ag@TiO₂ nanoparticles followed Chick's law and the pseudo first order rate constant was found to be 0.0426 min^{-1} for a catalyst loading of 0.1 g/L. Ag@TiO₂ was found to degrade endotoxin during photocatalytic disinfection of water wherein 72.5% endotoxin was degraded during solar photocataly-

sis with 1 g/L catalyst loading. The kinetics of endotoxin degradation follows zero order kinetics at high concentrations of endotoxin, but at lower concentrations rate follows a nth order model with a positive order. Ag@TiO₂ nanoparticles immobilized on cellulose acetate were found effective in solar disinfection, but with a lower rate than the free nanoparticles owing to diffusional and light penetration limitations. The re-growth of cells after photocatalytic disinfection was below the detectable limits, thus proving the potential of the process to produce safe drinking water. The nanoparticles were found to be photo catalytically active even in endotoxin degradation during photocatalytic disinfection. Disinfection of microbes and degradation of endotoxins occurred simultaneously thereby making the treated water safe for use. Ag@TiO₂ nanoparticles can find potential application in solar water disinfection and the process which harnesses the solar energy may prove to be energy efficient and economical, thus can be easily adopted for large scale applications and portable drinking water treatment units for domestic applications.

References

- Acra, Aftim, Karahagopian, Y., Raffoul, Z., Dajani, R., 1980. Disinfection of oral rehydration solutions by sunlight. *The Lancet* 316, 1257–1258.
- Bekbölet, M., 1997. Photocatalytic bactericidal activity of TiO₂ in aqueous suspensions of *E. coli*. *J. Water Sci. Technol.* 35, 95–100.
- Borges, M.E., Sierra, M., Cuevas, E., García, R.D., Esparza, P., 2016. Photocatalysis with solar energy: sunlight-responsive photocatalyst based on TiO₂ loaded on a natural material for wastewater treatment. *Sol. Energy* 135, 527–535.
- Chick, H., 1908. An Investigation of the laws of disinfection. *J. Hyg. (Lond.)* 8, 92–158.
- Cho, M., Chung, H., Choi, W., Yoon, J., 2004. Linear correlation between inactivation of *E. coli* and OH radical concentration in TiO₂ photocatalytic disinfection. *J. Water Res.* 38, 1069–1077.
- Choi, W., Termin, A., Hoffmann, M.R., 1994. The role of metal ion dopants in quantum-sized TiO₂: correlation between photoreactivity and charge carrier recombination dynamics. *J. Phys. Chem.* 98, 13669–13679.
- Dunlop, P.S.M., Byrne, J.A., Manga, N., Eggins, B.R., 2002. The photocatalytic removal of bacterial pollutants from drinking water. *J. Photochem. Photobiol. A Chem.* 148, 355–363.
- Galanos, C., Lehmann, V., Lüderitz, O., Rietschel, E.T., Westphal, O., Brade, H., Brade, L., Freudenberg, M.A., Hansen-Hagge, T., Lüderitz, T., 1984. Endotoxic properties of chemically synthesized lipid A part structures. Comparison of synthetic lipid A precursor and synthetic analogues with biosynthetic lipid A precursor and free lipid A. *Eur. J. Biochem* 140, 221–227.
- Gamage, M., 2014. Carbon-Enhanced Photocatalysts for Visible Light Induced Detoxification and Disinfection. Department of Chemical and Biological Engineering, University of Ottawa, Ottawa, Canada.
- Gelover, Silvia, Gómez, Luis A., Reyes, Karina, Leal, Ma Teresa, 2006. A practical demonstration of water disinfection using TiO₂ films and sunlight. *J. Water Res.* 40, 3274–3280.
- Gumy, D., Rincon, A.G., Hajdu, R., Pulgarin, C., 2006. Solar photocatalysis for detoxification and disinfection of water: different types of suspended and fixed TiO₂ catalysts study. *Sol. Energy* 80, 1376–1381.
- Gupta, S.M., Tripathi, M., 2011. A review of TiO₂ nanoparticles. *Chin. Sci. Bull.* 56, 1639–1657.
- Guzmán, M., Dille, J., Godet, S., 2009. Synthesis of silver nanoparticles by chemical reduction method and their antibacterial activity. *Int. J. Chem.* 2, 104–111.
- Gyüre, L.L., Finch, G.R., 1998. Modeling water treatment chemical disinfection kinetics. *J. Environ. Eng.* 124 (9), 783–793.
- Habibi, M.H., Hassanzadeh, A., Mahdavi, S., 2005. The effect of operational parameters on the photocatalytic degradation of three textile azo dyes in aqueous TiO₂ suspensions. *J. Photochem. Photobiol. A Chem.* 172, 89–96.
- Hirakawa, T., Kamat, P.V., 2004. Photoinduced electron storage and surface plasmon modulation in Ag@TiO₂ clusters. *Langmuir* 20, 5645–5647. <http://dx.doi.org/10.1021/ja048874c>.
- Hirakawa, T., Kamat, P.V., 2005. Charge separation and catalytic activity of Ag@TiO₂ core-shell composite clusters under UV-irradiation. *J. Am. Chem. Soc.* 127, 3928–3934.
- Huang, Z., Maness, P., Blake, D.M., Wolfrum, E.J., Smolinski, S.L., Jacoby, W.A., 2000. Bactericidal mode of titanium dioxide photocatalysis. *J. Photochem. Photobiol. A Chem.* 130, 163–170.
- Ibáñez, P.F., McGuigan, K.G., Mathur, C., Dhodapkar, R., Sawant, B., Joseph-Titus, C., Al-Eryani, Y.A., Calderero, F., Polo-López, M.I., Castro-Alferez, M., 2015. Capability of 19-L polycarbonate plastic water cooler containers for efficient solar water disinfection (SODIS): Field case studies in India, Bahrain and Spain. *Sol. Energy* 116, 1–11.
- Ibhadon, A., Fitzpatrick, P., 2013. Heterogeneous photocatalysis: recent advances and applications. *Catalysts* 3, 189–218.

- Kedziora, A., Streck, W., Kepinski, L., Bugla-Ploskonska, G., Doroszkiwicz, W., 2012. Synthesis and antibacterial activity of novel titanium dioxide doped with silver. *J. Sol-Gel. Sci. Technol.* 62, 79–86.
- Khanna, Ankita. 2014. Photocatalytic degradation of azo dyes using Ag core-TiO₂ shell structured nanoparticles Ph.D thesis. National Institute of Technology, Karnataka, Surathkal, India.
- Khanna, A., Shetty, K.V., 2013. Solar photocatalysis for treatment of acid yellow-17 (AY-17) dye contaminated water using Ag@TiO₂ core-shell structured nanoparticles. *Environ. Sci. Pollut. Res.* 20, 5692–5707.
- Khanna, A., Shetty, K.V., 2014. Solar light induced photocatalytic degradation of reactive blue 220 (RB-220) dye with highly efficient Ag@TiO₂ core-shell nanoparticles: a comparison with UV photocatalysis. *Sol. Energy* 99, 67–76.
- Khanna, A., Shetty, K.V., 2015. Solar light-driven photocatalytic degradation of Anthraquinone dye-contaminated water by engineered Ag@TiO₂ core-shell nanoparticles. *Desalin. Water Treat.* 54, 744–757.
- Lanao, M., Ormada, M.P., Gofñib, P., Miguela, N., Mosteoa, R., Ovelleiroa, J.L., 2010. Inactivation of clostridium perfringens spores and vegetative cells by photolysis and TiO₂ photocatalysis with H₂O₂. *Sol. Energy* 84, 703–709.
- Lanao, M., Ormad, M.P., Mosteoa, R., Ovelleiro, J.L., 2012. Inactivation of Enterococcus sp. by photolysis and TiO₂ photocatalysis with H₂O₂ in natural water. *Sol. Energy* 86, 619–625.
- Li, X.Z., Li, F.B., 2001. Study of Au/Au³⁺-TiO₂ photocatalysts toward visible photooxidation for water and wastewater treatment. *J. Environ. Sci. Technol.* 35, 2381–2387.
- Liga, M.V., Bryant, E.L., Colvin, V.L., Li, Q., 2011. Virus inactivation by silver doped titanium dioxide nanoparticles for drinking water treatment. *Water Res.* 45, 535–544.
- Mai, L., Wang, D., Zhang, S., Xie, Y., Huang, C., Zhang, Z., 2010. Synthesis and bactericidal ability of Ag/TiO₂ composite films deposited on titanium plate. *Appl. Surf. Sci.* 257, 974–978.
- Maness, P.C., Smolinski, S., Blake, D.M., Huang, Z., Wolfrum, E.J., Jacoby, W.A., 1999. Bactericidal activity of photocatalytic TiO₂ reaction: toward an understanding of its killing mechanism. *Appl. Environ. Microbiol.* 65, 4094–4098.
- Markad, G.B., Kapoor, S., Haam, S.K., Thakur, P., 2017. Metal free, carbon-TiO₂ based composites for the visible light photocatalysis. *Sol. Energy* 144, 127–133.
- Matsunaga, T., Tomoda, R., Nakajima, T., Wake, H., 1985. Photoelectrochemical sterilization of microbial cells by semiconductor powders. *FEMS Microbiol. Lett.* 29, 211–214.
- Miyamoto, T., Okano, S., Kasai, N., 2009. Inactivation of *Escherichia coli* endotoxin by soft hydrothermal processing. *Appl. Environ. Microbiol.* 75 (15), 5058–5063.
- Meierhofer, R., Wegelin, M., 2002. Solar water disinfection—a guide for the application of SODIS. Swiss Federal Institute of Environmental Science and Technology (EAWAG), Department of Water and Sanitation in Developing Countries (SANDEC) (ISBN 3-906484-24-6).
- Paleologou, A., Marakas, H., Nikolaos, P.X., Armando, M., Vergara, Y., Nicolas, K., Gikas, P., Dionissios, M., 2007. Disinfection of water and wastewater by TiO₂ photocatalysis, sonolysis and UV-C irradiation. *Catal. Today* 129, 136–142.
- Pham, H.N., Wilkins, E., Heger, A.S., Kauffman, D., 1997. Quantitative analysis of variations in initial *Bacillus pumilus* spore densities in aqueous TiO₂ suspension and design of a photocatalytic reactor. *J. Environ. Sci. Health A32* (1), 153–163.
- Pratap Reddy, M., Venugopal, A., Subrahmanyam, M., 2007. Hydroxyapatite-supported Ag-TiO₂ as *Escherichia coli* disinfection photocatalyst. *Water Res.* 41, 379–386.
- Pişkin, Sabriye, Palantöken, Arzu, Yılmaz, Müge Sari, 2013. Antimicrobial activity of synthesised TiO₂ nanoparticles. International Conference on Emerging Trends in Engineering and Technology, ICETET, Patong Beach, Phuket (Thailand).
- Qilin, L., Mahendra, S., Lyon, D.Y., Brunet, L., Liga, M.V., Li, D., Alvarez, P.J.J., 2008. Antimicrobial nanomaterials for water disinfection and microbial control: Potential applications and implications. *Water Res.* 42, 4591–4602.
- Richardson, S.D., Plewa, M.J., Wagner, E.D., Schoeny, R., DeMarini, D.M., 2007. Occurrence, genotoxicity, and carcinogenicity of regulated and emerging disinfection by-products in drinking water: a review and roadmap for research. *Mutat. Res. – Rev. Mutat. Res.* 636, 178–242.
- Rincón, A.G., Pulgarin, C., 2006. Comparative evaluation of Fe³⁺ and TiO₂ photoassisted processes in solar photocatalytic disinfection of water. *Appl. Catal. B Environ.* 63, 222–231.
- Rosenstreich, D.L., Nowotny, A., Chused, T., Mergenhagen, S.E., 1973. In vitro transformation of mouse bone marrow derived (B) lymphocytes induced by the lipid component of endotoxin. *Infect. Immun.* 8, 406–411.
- Sciaccia, F., Rengifo-Herrerac, J.A., Wéthéb, J., Pulgarina, C., 2011. Solar disinfection of wild *Salmonella* sp. in natural water with a 18 L CPC photoreactor: detrimental effect of non-sterile storage of treated water. *Sol. Energy* 85, 1399–1408.
- Sclafani, A., Herrmann, J.M., 1996. Comparison of the photoelectronic and photocatalytic activities of various anatase and rutile forms of Titania in pure liquid organic phases and in aqueous solutions. *J. Phys. Chem.* 100, 13655–13661.
- Shet, A., Shetty, K.V., 2015. Photocatalytic degradation of phenol using Ag core-TiO₂ shell (Ag@TiO₂) nanoparticles under UV light irradiation. *Environ. Sci. Pollut. Res. Int.* 23 (20), 20055–20064.
- Shet, A., Shetty, K.V., 2016. Solar light mediated photocatalytic degradation of phenol using Ag core-TiO₂ shell (Ag@TiO₂) nanoparticles in batch and fluidized bed reactor. *Sol. Energy* 127, 67–78.
- Sreeja, S., Shetty, V.K., 2016. Microbial disinfection of water with endotoxin degradation by photocatalysis using Ag@TiO₂ core shell nanoparticles. *Environ. Sci. Poll. Res.* 23 (18), 18154–181641.
- Sumana, B., Sarayu, K., Bruno, B., Udhaya, R., Sandhya, S., 2013. Solar light induced bactericidal activity of silver loaded TiO₂. *Int. J. Environ. Sci.* 4, 106–112.
- Sunada, K., Kikuchi, Y., Hashimoto, K., Fujishima, A., 1998. Bactericidal and detoxification effects of TiO₂ thin film photocatalysts. *Environ. Sci. Technol.* 32, 726–728.
- Sunada, K., Watanabe, T., Hashimoto, K., 2003. Studies on photokilling of bacteria on TiO₂ thin film. *J. Photochem. Photobiol. A Chem.* 156, 227–233.
- Tanaka, S., Aketagawa, J., Ohki, M., Takahashi, S., Tamura, H., Shibata, Y., 1992. US Patent number 5,155,032 (date of patent Oct 13 1992).
- Tunc, I., Bruns, M., Gliemann, H., Grunze, M., Koelsch, P., 2010. Bandgap determination and charge separation in Ag@TiO₂ core shell nanoparticle films. *Surf. Interface Anal.* 42, 835–841.
- Vivar, M., Pichel, N., Fuentes, M., 2017. Solar disinfection of natural river water with low microbiological content (10–10³ CFU/100 ml) and evaluation of the thermal contribution to water purification. *Sol. Energy* 141, 1–10.
- World Health Organization and UNICEF Joint Monitoring Programme (JMP), 2014. Progress on Drinking Water and Sanitation, 2014 Update.
- Wegelin, M., Canonica, S., Mechsner, K., Fleischmann, T., Pesaro, F., Metzler, A., 1994. Solar water disinfection: scope of the process and analysis of radiation experiments. *J. Water SRT – AQUA* 43, 154.
- Wu, L., Shamsuzzoha, M., Ritchie, S.M.C., 2005. Preparation of cellulose acetate supported zero-valent iron nanoparticles for the dechlorination of trichloroethylene in water. *J. Nanoparticle Res.* 7, 469–476.